

SUPPLEMENTARY INFORMATION for Rickheit et al.

SUPPLEMENTARY FIGURES

Suppl. Figure S1

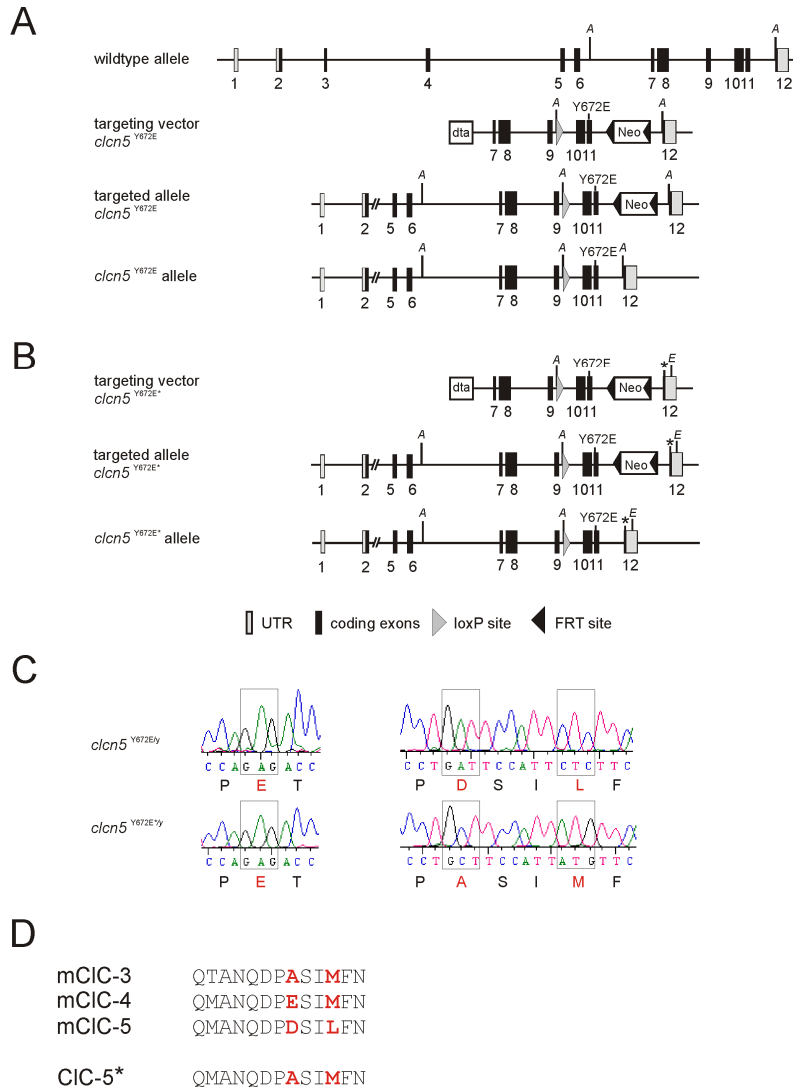


Fig. S1 Generation of CIC-5^{Y672E} knock-in mice and ‘negatively tagged’ CIC-5^{Y672E*} mice. *A* and *B*, Targeting strategies. Top, the targeting constructs containing 12.5 kb of mouse genomic *clcn5* sequence were modified by inserting the Y672E mutation into exon 11 (*A* and *B*) and by changing four base pairs in exon 12 that mutate two amino-acids of the extreme carboxy-terminus (indicated by an asterisk ‘*’, *B*). For positive selection a FRT flanked neomycin-resistance cassette was inserted into intron 11 and for negative selection a diphtheria toxin A (*dta*) cassette was added at the 5’ end. In addition, an *Acc65I* (A) site (with a loxP site) was inserted into intron 9 and an *EcoRV* site was added in the 3’UTR for screening purposes (*A* and *B*). *In vivo* Flp-mediated deletion of the neomycin-resistance cassette resulted in the *clcn5*^{Y672E} (*A*, bottom) and *clcn5*^{Y672E*} (*B*, bottom) alleles. *C*, Confirmation of inserted point mutations by sequencing PCR-amplified genomic DNA from WT, *clcn5*^{Y672E} and *clcn5*^{Y672E*} mice. *D*, Alignment of endosomal CLCs highlighting the position of corresponding amino acids that were exchanged to generate the ‘negative tag’ (*) in CIC-5.

Suppl. Figure S2

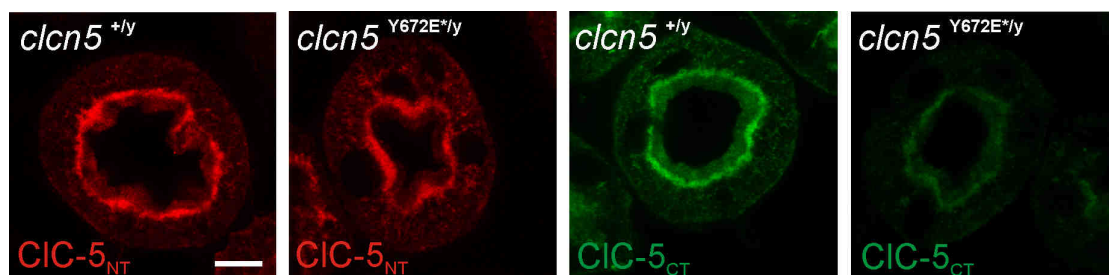


Fig. S2 Localization of CIC-5^{Y672E*} in kidney proximal tubules by immunohistochemistry. ‘Negatively tagged’ CIC-5^{Y672E*} is strongly recognized by an N-terminal CIC-5 antibody (red) but only faintly by a C-terminal CIC-5 antibody (green), contrasting with WT CIC-5. L: intestinal lumen. Scale bar, 10 μ m.

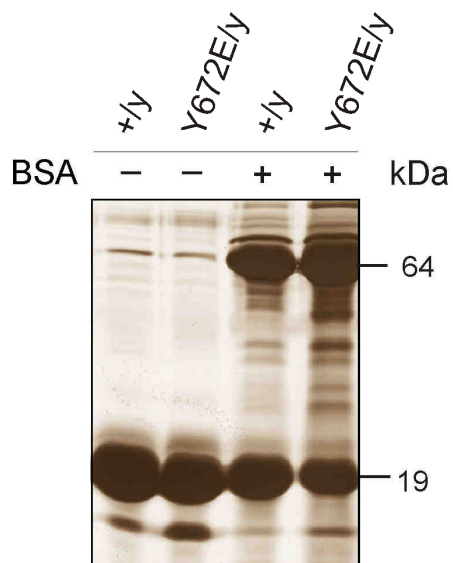
Table S3

urine concentrations (mmol/mmol creatinine)	<i>clcn5</i> ^{+/y}	<i>clcn5</i> ^{Y672E/y}
P _i	13.13 (\pm 1.52)	15.52 (\pm 1.62)
Na ⁺	47.16 (\pm 3.36)	49.80 (\pm 2.19)
K ⁺	131.65 (\pm 6.69)	126.54 (\pm 2.46)
Cl ⁻	61.11 (\pm 2.97)	59.14 (\pm 1.11)
Mg ²⁺	6.93 (\pm 0.48)	7.09 (\pm 0.54)
Ca ²⁺	3.9 (\pm 0.35)	4.26 (\pm 0.61)
creatinine (mmol/l)	2.93 (\pm 0.18)	2.82 (\pm 0.19)
urea (mmol/l)	1.52 (\pm 0.07)	1.41 (\pm 0.08)

Table S3 Urine parameters of WT and CIC-5^{Y672E} mice. Standard urine parameters were determined in urine of WT and CIC-5^{Y672E} male mice and adjusted to creatinine values. No significant differences between genotypes were detected. (11 animals per genotype; \pm SEM)

Suppl. Figure S4

A



B

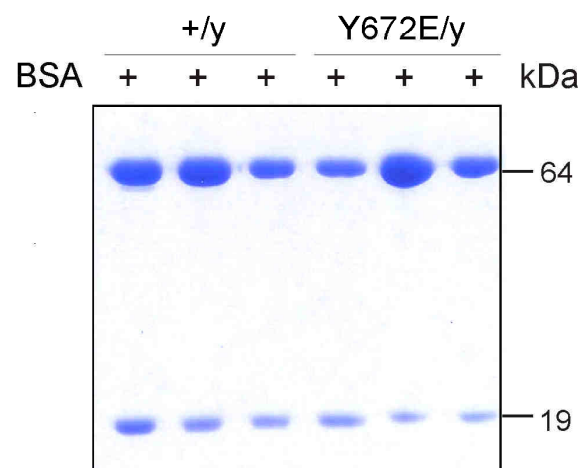


Fig. S4 Urinary proteins after induction of albuminuria in WT and $CIC-5^{Y672E}$ mice. A, Silver-staining of urine before (-) and after (+) induction of albuminuria by intraperitoneal injection of bovine serum albumin (BSA) into WT and $CIC-5^{Y672E}$ male mice. B, Coomassie staining of urinary proteins from albumin-injected mice reveals albumin (upper band) and the major urinary protein (lower band) in both WT and $CIC-5^{Y672E}$ mice. No difference between genotypes was detected before and upon induction of albuminuria. Similar results were obtained with 6 animals per genotype.

Suppl. Figure S5

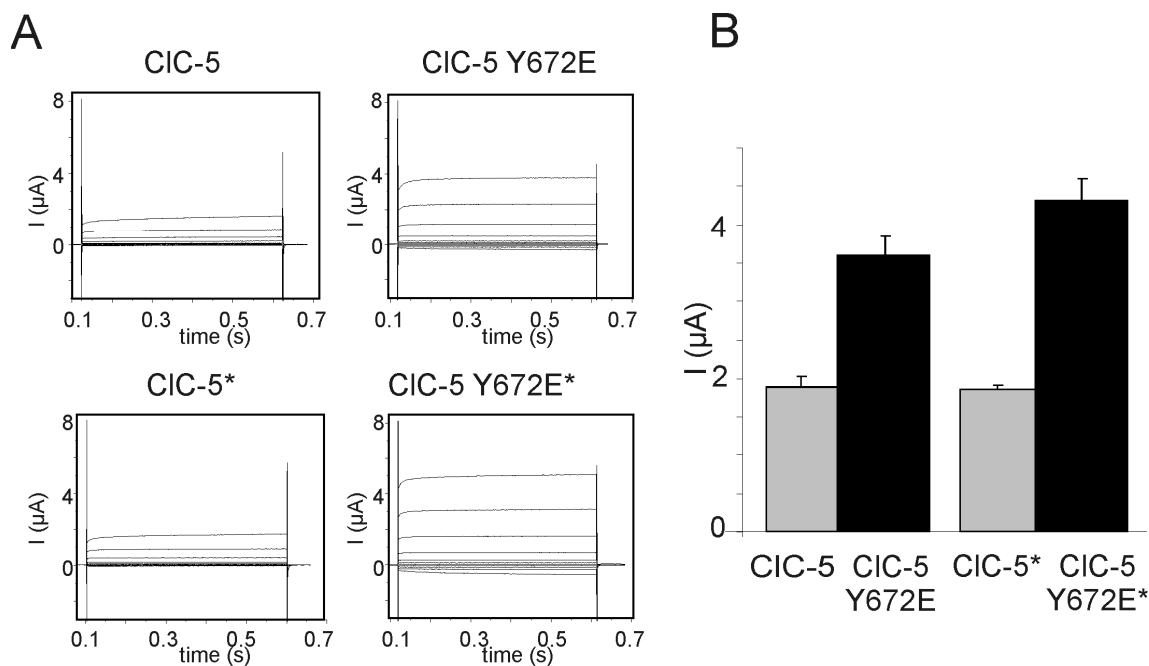


Fig. S5 Introducing a ‘negative tag’ by changing the C-terminus of CIC-5 to that of CIC-3 does not interfere with the enhancement of currents by the PY mutant.

A, CIC-5, CIC-5*, CIC-5^{Y672E} and CIC-5^{Y672E*} were expressed in *Xenopus* oocytes and currents measured by two-electrode voltage-clamp. Typical original traces show that both, CIC-5^{Y672E} and CIC-5^{Y672E*} yield approximately 2-fold increased currents when compared to CIC-5 or CIC-5* and retain the characteristic CIC-5 current properties. B, Mean currents at +100 mV indicate that the conversion of the C-terminus into CIC-3 does not influence CIC-5 current properties (n=10, \pm SEM).

Suppl. Figure S6

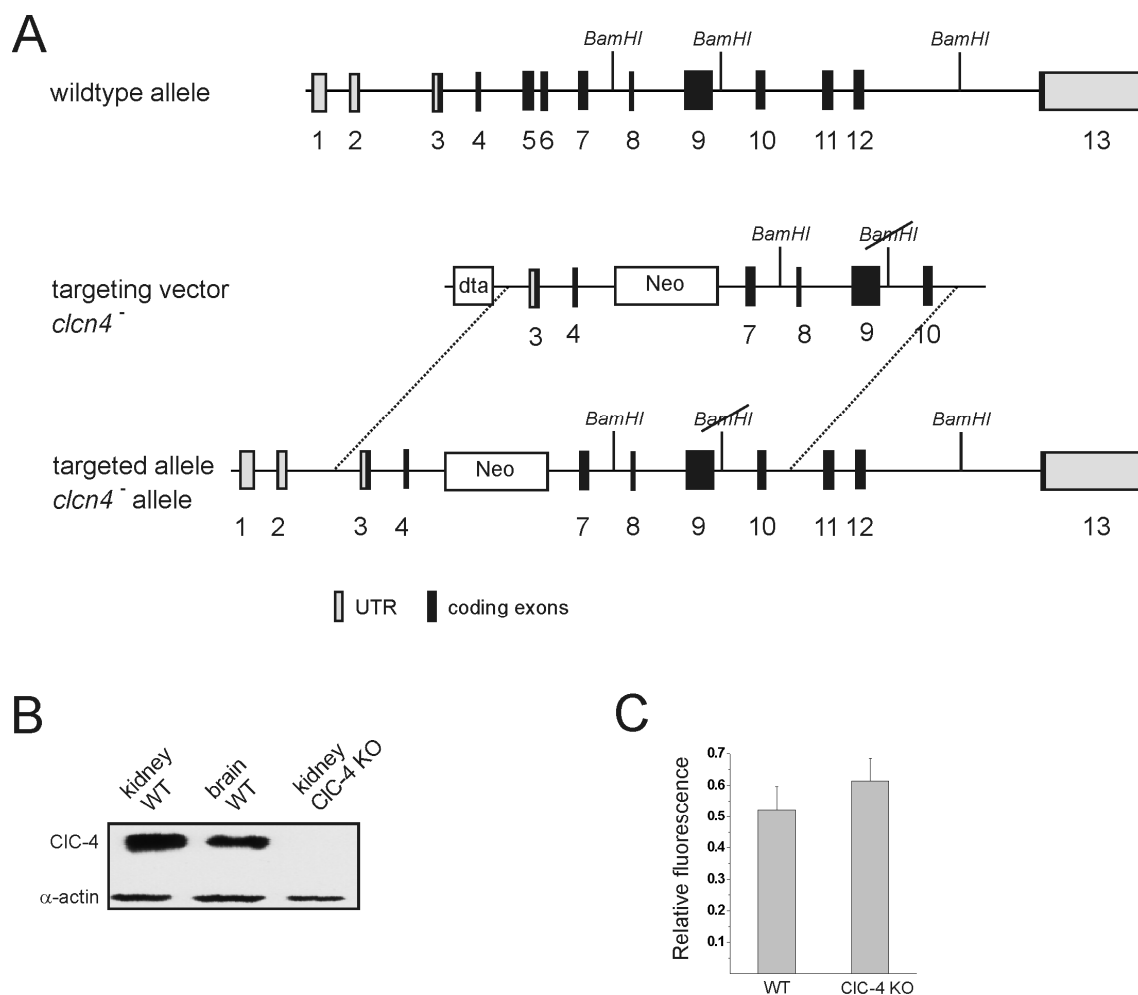


Fig. S6 Generation of a CIC-4 knock-out mouse model. *A*, Targeting strategy. Top, Mouse genomic *cln4* sequence encompassing 13 exons. Middle, To generate the targeting construct, 12.2 kb *cln4* sequence (containing exons 1-11) from a genomic lambda phage library were isolated. In the targeting construct, exons 5 and 6 were replaced by a neomycin-resistance cassette for positive selection. Further, a diphtheria toxin A (dta) cassette for negative selection was inserted into the 5' sequence before exon 3. For screening purposes, a *Bam*HI site in intron 9 was eliminated by mutation. Bottom, Homologous recombination between the targeting construct and the endogenous *cln4* allele gave the CIC-4 KO allele. In *cln4*^{-/-} mice, loss of exons 5 and 6 cause a shift of the open reading frame. *B*, Immunoblot for CIC-4 using kidney and brain homogenates of WT and CIC-4 KO mice with an antibody against CIC-4 shows no CIC-4-specific signal in KO lysates. *C*, The fluorescence of endocytosed Alexa Fluor 488-labeled 10kDa dextran was quantified in kidney homogenates 15 min after injection into the vena cava and subsequent flushing with PBS. No significant difference in the amount of endocytosed dextran between WT and *cln4*^{-/-} mice was detected (numbers of animals: 8 WT, 10 KO). Error bars SEM.

Suppl. Figure S7

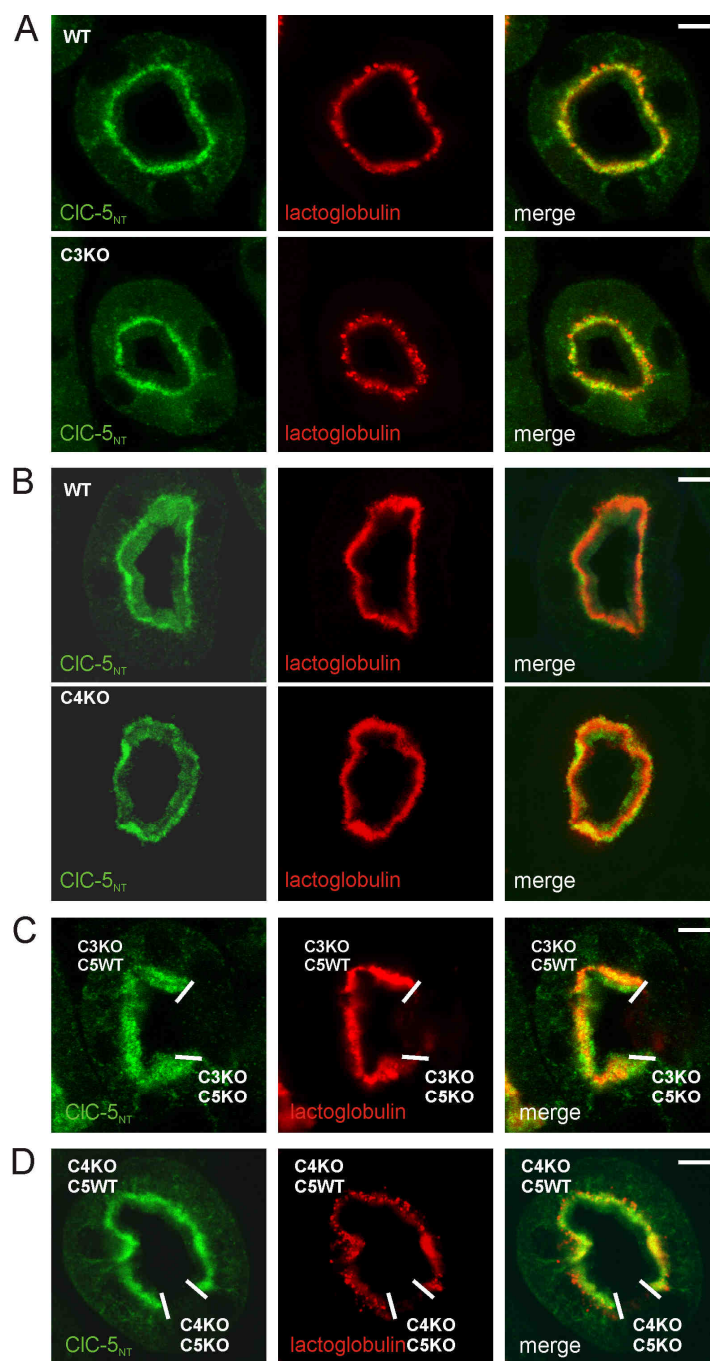


Fig. S7 Neither CIC-4 nor CIC-3 compensate for CIC-5 endocytic function in proximal tubules. Mice were injected with Alexa-dye-labeled β -lactoglobulin or dextran (both red) to examine receptor-mediated or fluid-phase endocytosis, respectively, and were fixed 10 min after injection. Cryo-sections were immunostained with an N-terminal anti-CIC-5 antibody (green). *A* and *B*, No difference in endocytosis of β -lactoglobulin or dextran was observed between WT and *cln3*^{-/-} (C3KO) mice (*A*) or WT and *cln4*^{-/-} (C4KO) mice (*B*). *C* and *D*, Additional depletion of CIC-3 (*C*) or CIC-4 (*D*) in the CIC-5 knock-out background (*C*: *cln3*^{-/-}; *cln5*^{lox/y}; villin-cre; *D*: *cln4*^{-/-}; *cln5*^{lox/y}; villin-cre mice) did not aggravate the reduction in endocytic uptake of β -lactoglobulin observed upon loss of CIC-5 (Piwon et al., *Nature* **408**, 369-373 (2000)). Scale bars 20 μ m.

Suppl. Figure S8

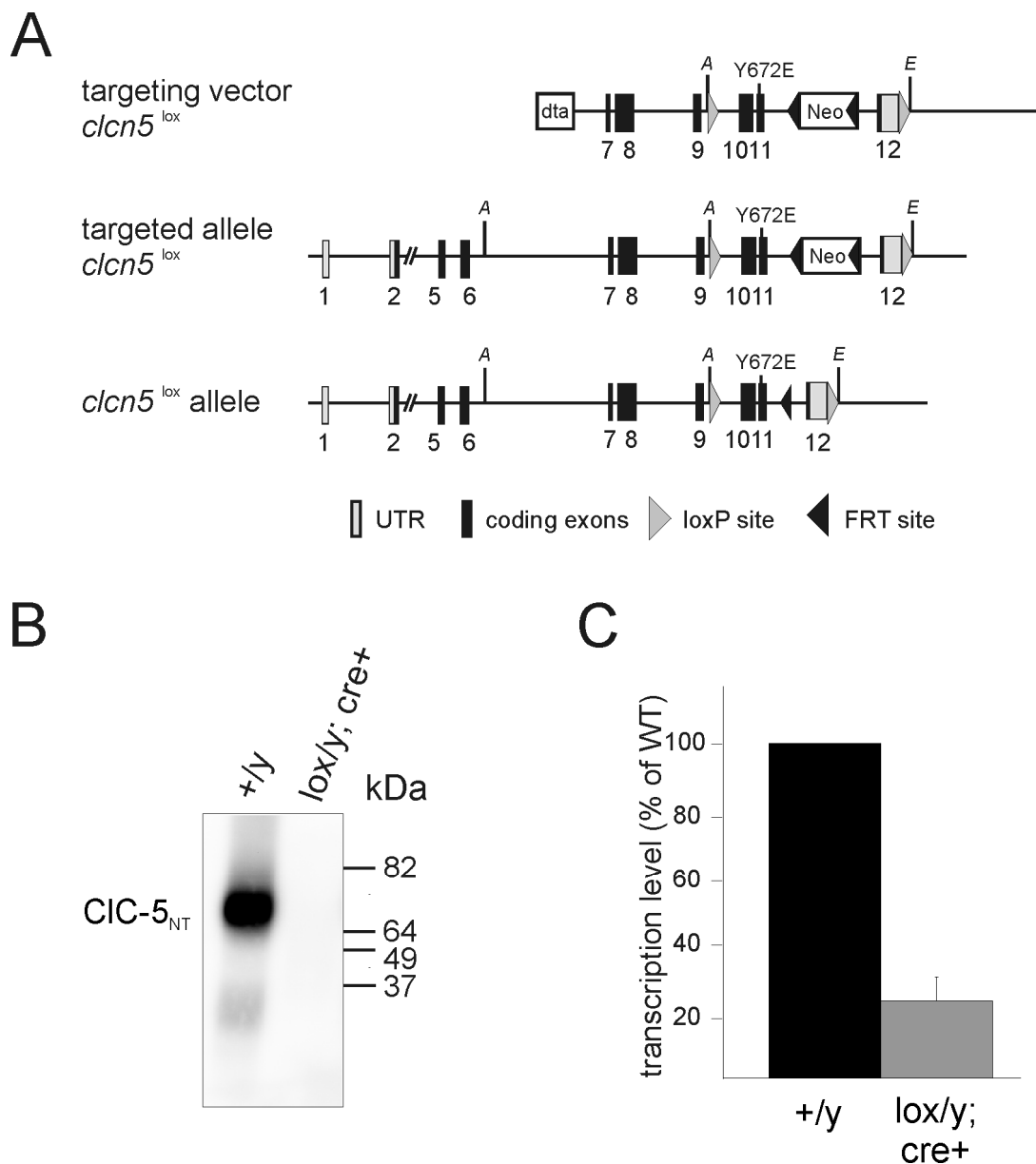


Fig. S8 Generation of a conditional CIC-5 knock-out mouse model. *A*, Targeting strategy. Top, targeting construct containing 12.5 kb of mouse genomic sequence that has been modified by flanking exons 10 to 12 with loxP sites. Additionally, a FRT flanked neomycin-resistance cassette has been inserted into intron 11, and a diphtheria toxin A (dta) cassette has been added to the 5' end for negative selection. For screening purposes, an *Acc65I* site (A) has been inserted close to the proximal loxP site and an *EcoRV* site has been added close to the distal loxP site. Flp-mediated deletion of the neomycin-resistance cassette *in vivo* resulted in the conditional *clcn5*^{lox} allele (bottom). *B*, Immunoblot for CIC-5 using kidney lysates of WT and *clcn5*^{lox};cre mice (equivalent to a complete CIC-5 KO) that were obtained by crossing *clcn5*^{lox} mice with the *deleter-cre* line (Schwenk et al., *Nucleic Acids Res* **23**, 5080-5081 (1995)), with an antibody against the N-terminus shows no CIC-5-specific signals in KO lysates. No truncated CIC-5 protein can be detected. *C*, Quantitative real-time PCR on total RNA extracted from WT and *clcn5*^{lox/y};cre kidneys shows drastically reduced CIC-5 mRNA levels in *clcn5*^{lox/y};cre mice. (n=3, ± SEM).

SUPPLEMENTARY METHOD

Expression in *Xenopus* oocytes and voltage clamp analysis

CIC-5 constructs were cloned into PTLN oocyte expression vector (Lorenz et al., *PNAS* **93**, 13362-13366 (1996)). 5 ng of cRNA was injected into defolliculated *Xenopus laevis* oocytes which were then kept at 17°C in ND96 solution (containing 96 mM NaCl, 2mM KCl, 1.8 mM CaCl₂, 1mM MgCl₂, 5 mM HEPES, pH 7.5). Standard two-electrode voltage clamp measurements were performed as described (Steinmeyer et al., *J Biol Chem* **270**, 31172-31177 (1995); Friedrich et al., *J Biol Chem* **274**, 896-902 (1999)) at room temperature two days after injection using a Turbotec10C amplifier (NPI Instruments) and pClamp8 software (Axon Instruments). Currents were recorded in ND96 solution.